THE NRF-2 ACTIVATOR DH404 ATTENUATES ADVERSE VENTRICULAR REMODELLING POST-MYOCARDIAL INFARCTION BY MODIFYING REDOX SIGNALLING

*Kristen J Bubb[1], *Cindy Kok[1], , Owen Tang[1], Nathalie B Rasko[1], Asa Birna Birgisdottir[1,5], Thomas Hansen[1], Rebecca Ritchie[2], Ravinay Bhindi[1,4], Scott A Reisman[3], Colin Meyer[3], Keith Ward[3], Keyvan Karimi Galougahi[1], Gemma A Figtree[1,4].

*These authors contributed equally.

1. North Shore Heart Research Group, Kolling Institute, University of Sydney, Australia
2. Baker IDI Heart and Diabetes Institute, Melbourne, Australia
3. Reata Pharmaceuticals, Inc. Irving, TX, USA
4. Department of Cardiology, Royal North Shore Hospital and University of Sydney, Australia
5. Molecular Cancer Research Group, Institute of Medical Biology, University of Tromsø, 9037 Tromsø, Norway.

Corresponding author:
Professor Gemma Figtree MBBS DPhil (Oxon) FRACP FAHA
North Shore Heart Research Group
Kolling Institute, University of Sydney and Royal North Shore Hospital
Sydney, AUSTRALIA
Email: gemma.figtree@sydney.edu.au
Phone +612 9926 4915

Abstract

Background: The novel synthetic triterpenoid, bardoxolone methyl, has the ability to upregulate cytoprotective proteins via induction of the nuclear factor erythroid-2-related factor 2 (Nrf2) pathway. This makes it a promising therapeutic agent in disease states characterized by dysregulated oxidative signalling. We have examined the effect of a Nrf2 activator, dihydro-CDDO-trifluoroethyl amide (DH404), a derivative of bardoxolone methyl, on post-infarct cardiac remodeling in rats. **Methods/Results:** DH404, administered from day 2 post myocardial infarction (MI: 30 min transient ischemia followed by reperfusion) resulted in almost complete protection against adverse ventricular remodeling as assessed at day 28 (left ventricular end-systolic area: sham 0.14±0.01 cm^2, MI vehicle 0.29±0.04 cm^2 vs. MI DH404 0.18±0.02 cm^2, $P<0.05$) ; infarct size (21.3±3.4 % MI vehicle vs. 10.9±2.3 % MI DH404, $P<0.05$) with associated benefits on systolic function (fractional shortening: sham 71.9±2.6%, MI vehicle 36.2±1.9% vs. MI DH404 58.6±4.0%, $P<0.05$). These structural and functional benefits were associated with lower myocardial expression of atrial natriuretic peptide (ANP, $P<0.01$ vs. MI vehicle), and decreased fibronectin ($P<0.01$ vs. MI vehicle) in DH404-treated MI rats at 28 days. MI increased glutathionylation of endothelial nitric oxide synthase (eNOS) *in vitro* - a molecular switch that uncouples the enzyme, increasing superoxide production and decreasing nitric oxide (NO) bioavailability. MI-induced eNOS glutathionylation was substantially ameliorated by DH404. An associated increase in glutaredoxin 1 (Grx1) co-immunoprecipitation with eNOS without a change in expression was mechanistically intriguing. Indeed, in parallel in vitro experiments, silencing of Grx1 abolished the protective effect of DH404 against Angiotensin II-induced eNOS uncoupling. **Conclusion:** The bardoxolone derivative DH404 significantly attenuated cardiac remodeling post MI, at least in part, by re-coupling of

eNOS and increasing the functional interaction of Grx1 with eNOS. This agent may have clinical benefits protecting against post MI cardiomyopathy.

Graphical abstract

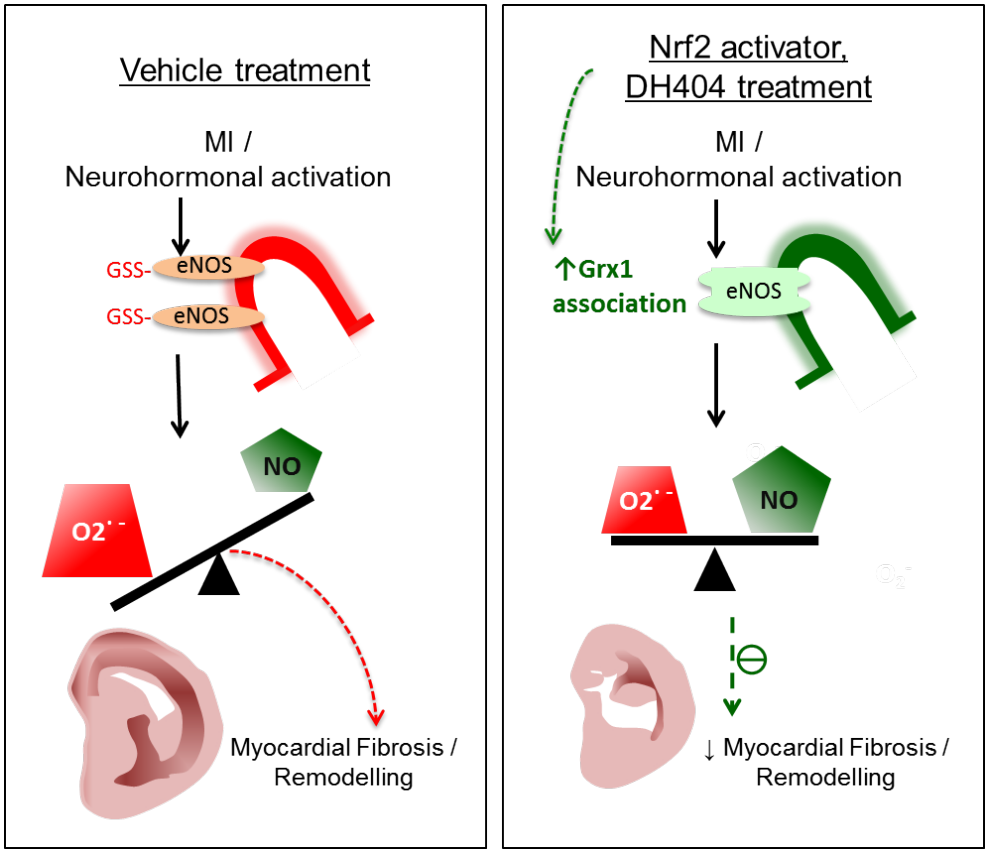

Highlights

- The bardoxolone derivative DH404 reduced adverse cardiac remodeling post myocardial infarction
- Oral DH404 improved markers of heart failure and fibrosis post myocardial infarction
- DH404 increased functional association of glutaredoxin with eNOS
- Protection against eNOS glutathionylation is a new mechanism of DH404 benefit
- Bardoxolone has potential therapeutic role in ST elevation MI patients

Keywords: bardoxolone, endothelial nitric oxide synthase, heart failure, caveolae, glutaredoxin

Abbreviations: AngII, angiotensin II; ANOVA, analysis of variance; ANP, atrial natriuretic peptide; DH404, dihydro-CDDO-trifluoroethyl amide; eNOS, endothelial nitric oxide synthase; Grx1, glutaredoxin 1; GSS, glutathionylation; Keap1, Kelch-like erythroid cell-derived protein with CNC homology-associated protein 1; LCA, Left coronary artery; LV, left ventricle; MI, Myocardial infarction; NO, nitric oxide; Nrf2, nuclear factor erythroid-2-related factor 2; Nqo1, NADPH quinone oxidoreductase 1; PCR, polymerase chain reaction; ROS, reactive oxygen species; SEM, standard error of mean; SERCA-2, sarco-endoreticuloplasmic Ca^{2+} ATPase 2A;

Introduction

Ischemic heart disease remains the number one cause of death in adults [1]. Major advances have been made in rapid restoration of epicardial blood flow to jeopardized myocardium at the time of coronary occlusion, substantially reducing mortality from MI. However, adverse myocardial remodeling post MI contributes to substantial morbidity including heart failure and arrhythmia [2].

Reactive oxygen species (ROS) are known to play an important role in triggering molecular signalling events that drive adverse remodeling post MI and reperfusion [3, 4], with additional contributory factors including elevated intracellular sodium levels [5], calcium dysregulation, endothelial dysfunction [6], mitochondrial dysfunction, inflammation and apoptosis [4]. Initially, the production of ROS results from the reintroduction of molecular oxygen into a previously ischemic tissue. Beyond this, ROS are generated from damaged components of the mitochondrial electron transport chain, from activation of cellular enzymes such as nicotinamide adenine dinucleotide phosphate (NADPH) oxidases, and uncoupled NO synthases and from neutrophil activation [7]. Free radicals contain an unpaired electron and are highly reactive with cellular phospholipids and proteins. They are particularly disruptive to membrane proteins and ultrastructure [3], with their specific effects dependent on their site of production and cellular compartmentalization.

Despite the pathophysiological role of ROS in MI and heart failure, trials of oxygen free radical scavengers or general antioxidants have seen limited success. General antioxidant therapies, such as superoxide dismutase/catalase combinations [8, 9], or vitamin E analogues [10], have failed to translate to clinically useful therapies that reduce cardiovascular morbidity and mortality. This likely relates to their inability to

alter the focal concentration of ROS in cellular micro domains, such as caveolae, during key cellular signalling events.

Bardoxolone methyl is an orally available synthetic triterpenoid that belongs to a so-called class of drugs 'antioxidant inflammation modulators'. These drugs have the potential to overcome the limitations of previously trialed antioxidant strategies, by their ability to enhance endogenous cellular protective mechanisms. They are among the most potent activators of Nrf2 [11]. Through their interaction with cysteine residues on Kelch-like erythroid cell-derived protein with CNC homology-associated protein 1 (Keap1), bardoxolone methyl and similar triterpenoids facilitate the nuclear translocation of Nrf2 [12, 13]. This results in Nrf2 complexes binding to regulatory gene regions called antioxidant response elements (ARE) [14, 15] leading to the up-regulation of numerous antioxidant and anti-inflammatory proteins [16]. In addition, bardoxolone is a potent inhibitor of the nuclear factor-kB inflammatory pathway [17]. These cellular benefits have led to extensive preclinical and clinical studies of bardoxolone in chronic kidney disease, including a positive phase 2 clinical trial in patients with advanced chronic kidney disease [18]. However, the effects of bardoxolone in the heart have not been studied in detail. One of the few published articles on the cardiovascular effects of Nrf2 upregulation, used an alternative synthetic triterpenoid derivative, DH404. This study demonstrated that DH404 suppressed angiotensin II (AngII)-induced oxidative stress in cultured cardiomyocytes [19]. Another showed that pressure overload-induced heart failure can be alleviated by DH404 [20]. In this study, we have examined the effects of Nrf2 activation via the administration of DH404 on ischemic ventricular remodeling in a rat model of MI.

Methods

Animal studies and MI model: The study was approved by the Northern Sydney Local Health District Animal Ethics Committee (approval number 1210-016A) and conforms to the National Health and Medical Research Council of Australia's *Code of Practice for the Care and Use of Animals for Scientific Purposes*. Experiments were performed in male Sprague Dawley rats (250-350 g).

MI model in rats

To mimic the clinical scenario of primary percutaneous intervention for ST elevation MI (STEMI), a model of transient coronary ligation, followed by reperfusion was used. Initial studies demonstrated that, even with 2 days preloading, DH404 had no effect on MI size 2 days post-MI, when measured by infarct area normalized to the area at risk by Evan's blue stain (data not shown). Given this result, and the fact that it is not practical in the clinical situation to administer a potentially protective agent for the days prior to an MI, we focused on the potential therapeutic effect of DH404 in the remodeling phase from day 2 to 28 post MI. Rats were anaesthetized with 2% isoflurane vaporized in oxygen, delivered via a nose-cone at 1.0 l/min. Endo-tracheal intubation was performed using a 16-gauge intravenous catheter after direct visualization of the vocal cords and ventilation was applied (80 breaths/min tidal volume; 1.5 ml/100 g body weight) using a small animal ventilator. The chest was opened at the left 5th intercostal space with the incision parallel to the ribs, exposing the heart. The pericardium was opened, taking care not to injure the epicardium. The left coronary artery (LCA) was visualized and ligated using a 5/0 Prolene suture, which was passed through the myocardium deep to the vessel as described previously [21], and secured

~2 to 3 mm distal to the junction of pulmonary artery and left atrial appendage to create transient ligation. After 30 minutes the ligature was released and an 18-gauge intravenous chest tube used to create negative intra-thoracic pressure. The animals were then hyperventilated to assist in lung reflation prior to final chest closure with layered sutures. Lignocaine (10mg/kg i.m) was administered pre-surgery and 2 hours post-surgery to assist in preventing arrhythmias. In the sham procedure group, the suture was passed underneath the LCA but not tightened. Rats were allowed to recover, with administration of buprenorphine (0.1 mg/kg, s.c.) as required and ampicillin (100mg/kg, s.c) at the end of surgery. Rats were culled at 28 days post MI.

DH404 preparation and dosing: DH404 was dissolved in sesame oil and administered daily via oral gavage at 10 mg/kg/day for 26 days from the second day post MI. Vehicle controls received sesame oil only. The dosage and frequency was based upon experience of REATA pharmaceuticals in rodent dosing of DH404.

Echocardiography: Animals underwent echocardiography measurements 1 day prior to commencement of DH404 treatment, immediately before the surgical procedure and at 2, 7, 14 and 28 days post-surgery. Anesthesia was induced using vaporized 2% isoflurane and maintained using a nose-cone. Parasternal short axis views of the left ventricle (LV) were recorded and used to calculate LV systolic and diastolic dimensions and LV ejection fraction as indexes of cardiac remodeling in response to MI.

Assessment of MI: Heart sections (5 μm) from five levels, sectioned on the short axis were stained with Milligan's trichrome and imaged using light microscopy. The

circumference of the fibrotic infarct area was measured using Image J software (NIH Image) and normalized for left ventricle size as previously described [22]. Picrosirius red staining plus polarized light microscopy were used to detect collagen and this was quantified in regions of interest similar to the Milligan's trichrome stain [23].

Messenger RNA quantification. Total RNA was isolated from whole heart homogenate using Qiagen RNA extraction minikit (Qiagen, Australia) with DNase treatment step and quantified using nanodrop spectrophotometry (Thermofisher, Australia). 1 μg of RNA was converted to cDNA using Tetro cDNA synthesis kit (Bioline, Australia). For quantitative real-time polymerase chain reaction (PCR) template cDNA was added to FastStart Universal SYBR Green Mastermix (ROX) with ANP (forward primer 5' GAGGAGAAGATGCCGGTAG 3'; reverse primer 5' TCAGAGAGGGAGCTAAGTG 3'), fibronectin (forward primer 5' GGGATCAAAGGGAAACACAG 3'; reverse primer 5' AGACGGCAAAAGAAAGCAG 3') and qPCR was performed over 40 cycles using ABI7900HT (Applied Biosystems, Australia). Gene expression was normalized to expression of β-actin (forward primer 5' CCCGCGAGTACAACCTTCT 3'; reverse primer 5' CGTCATCCATGGCGAACT 3') and analysed using $2^{-\Delta\Delta Ct}$[24]. Grx1 (forward primer 5' CTGTCAGCATGGCTCAGGAGT 3'; reverse primer 5' CCACAAATTCCAGGAGACCAC 3' expression was detected by reverse transcriptase PCR using Superscript III ® (Invitrogen, USA). For Nrf2 target genes, mRNA was quantified as previously described using the Quantigene™ Plex 2.0 assay from Affymetrix (Santa Clara, CA) [25]. A modified multiplex panel (Catalog # 331173) with targets designed against the rat genome was used. A description of the panel with accession numbers can be found at https://www.ebioscience.com/application/gene-expression/quantigene-plex-

assay.htm. The mRNA expression data were standardized to the internal control ribosomal protein l19 (Rpl19) and presented as fold the mean vehicle control.

Immunoprecipitation: Hearts isolated from the experimental animals were snap-frozen and homogenized in ice-cold lysis buffer containing 150 mM NaCl, 200 mM Tris-HCl (pH 8.0), 1% Triton X-100, 0.5% Deoxycholic acid, 0.1% SDS and, and protease inhibitors (cOmplete™ EDTA-free, Roche Diagnostics). 500 µg of protein lysate was used for the co-immunoprecipitation with eNOS by incubating samples with protein G dynabeads (1.5 mg/ml, 2.8 µm beads, Thermofisher Scientific, Australia) conjugated with anti-eNOS antibody (BD Biosciences, 1 µg). Samples were denatured and run on SDS-PAGE and transferred onto polyvinylidene fluoride membrane and the amount of glutathionylated eNOS was determined by immunoblotting under non-reducing conditions with anti-glutathione antibody (Virogen, 1:500). Anti-fibronectin (BD biosciences, 1:1000) and anti-Grx1 (Abcam, 1:500) were detected under reducing conditions. Anti-glutathione was used for detecting total glutathionylation under non-reducing conditions using Licor Odyssey Western blotting with fluorescent anti-mouse secondary antibodies. H9C2 rat cardiomyocytes (ATCC, Australia) were grown to ~50% confluence in DMEM supplemented with 10% fetal bovine serum and penicillin/streptomycin (50 U/ml penicillin and 0.5 mg/ml streptomycin) before exposure to AngII (500nmol/l) and either vehicle (0.01% dimethyl sulfoxide) or DH404 (200 nmol/l) for 24 hours. Cells were lysed in NP-40 buffer (NaCl 150 mmol/l, Tris-Cl 50 mmol/l, pH 8.0, NP-40 1%) for optimal preservation of protein-protein associations. 500 µg protein lysate was used for eNOS-Grx1 co-immunoprecipitation under reducing conditions. Lysate was also incubated with mouse IgG as a negative control [26, 27].

NO and superoxide detection: Intracellular levels of nitric oxide in living cells were detected using 4-Amino-5-Methylamino-2',7'-Difluorofluoroscein Diacetate (DAF-FM; 1 μmol/l) and $O_2^{\cdot-}$ levels were detected using dihydroethidium (DHE; 2 μmol/l) according to manufacturer's instructions (Thermofisher Scientific, Australia). H9C2 cells were grown to ~50-70% confluence on glass coverslips before treatment with either AngII (500 nmol/l) + 0.01% DMSO vehicle or AngII + DH404 (200 nmol/l) for 24 hours in DMEM medium with 0.5 % serum. Media was replaced with physiological saline solution containing 2.5 mmol/L calcium chloride and DAF-FM or DHE (in presence or absence of superoxide dismutase mimetic, MnTMPyP, 30 μmol/L) was then added for 30 minutes in before cells were washed and fixed in 4% paraformaldehyde. The fixed cells on coverslips were mounted on glass slides with ProLong Diamond Antifade Mountant with DAPI (Thermofisher Scientific, Australia). Confocal images were collected with a 40 x oil objective (Leica Microsystems, Germany) to detect DAF-FM or DHE staining at an excitation/emission maxima of 495/515 nm (DAF-FM) or 518/605 nm (DHE). In some experiments, 24 hours prior to treatment with AngII ± DH404, cells were transfected with either rat non-specific siRNA (Mission® Universal negative control, Sigma Aldrich, Australia) or rat Grx1 siRNA (SASI_Rn01_00108522; Sigma Aldrich, Australia) at 0.3 μmol/l using Lipofectamine 2000 transfection reagent (3.75 μg, Invitrogen, USA) in OptiMEM, according to manufacturer´s recommendations. For each condition 6 fields were randomly chosen per experiment for image capturing and total fluorescence per field was quantified and normalized to cell number using Leica imaging software.

Statistical analysis: Data are expressed as mean ± standard error of the mean (SEM). Calculations were performed using unpaired Student's t-test for comparing two groups, or by one-way analysis of variance (ANOVA) with Bonferroni post-hoc analysis for

multiple comparisons. Data not normally distributed were tested using non-parametric Mann-Whitney or Kruskal-Wallis with Dunn's correction tests. A P value <0.05 was considered statistically significant.

Results

Effect of DH404 on ventricular remodeling post MI

We examined the effect of DH404 on ventricular remodeling using a rat model of MI. In our hands, temporary ligation of the LCA for 30 minutes results in a reproducible degree of MI of 35.6±2.6 % of the area at risk two days post MI surgery. This resulted in a drop in fractional shortening at the mid-ventricular level from 64.7±2.4 % pre-surgery to 50.5±2.7 % 2 days post MI (n=16, P=0.0005 Student's t-test). At this point, treatment with DH404 or vehicle commenced and continued to 28 days post MI. There was no effect of DH404 on LV dimensions or contractility in the sham-treated animals. However, DH404 exerted a protective effect on the post MI ventricular remodeling as demonstrated by improved fractional shortening and smaller end-systolic area on serial echocardiography compared with vehicle-treated MI rats (Figure 1). Whereas the MI animals receiving vehicle control had an almost doubling of the end-systolic area by day 28, those receiving DH404 were resilient to this increase (Figure 1A, B). The protective effect of DH404 on end-systolic area was significant from day 14, greatest at day 28 (Figure 1A,B); and was associated with almost complete return to pre-MI systolic function (Figure 1E,F: 60.2 ± 4.1% at day 28 vs. pre-MI of 64.3 ± 4.5%; vs. 36.2 ± 1.9 % at day 28 in vehicle-treated MI rats). End-diastolic areas were not affected by DH404 treatment (Figure 1C, D).

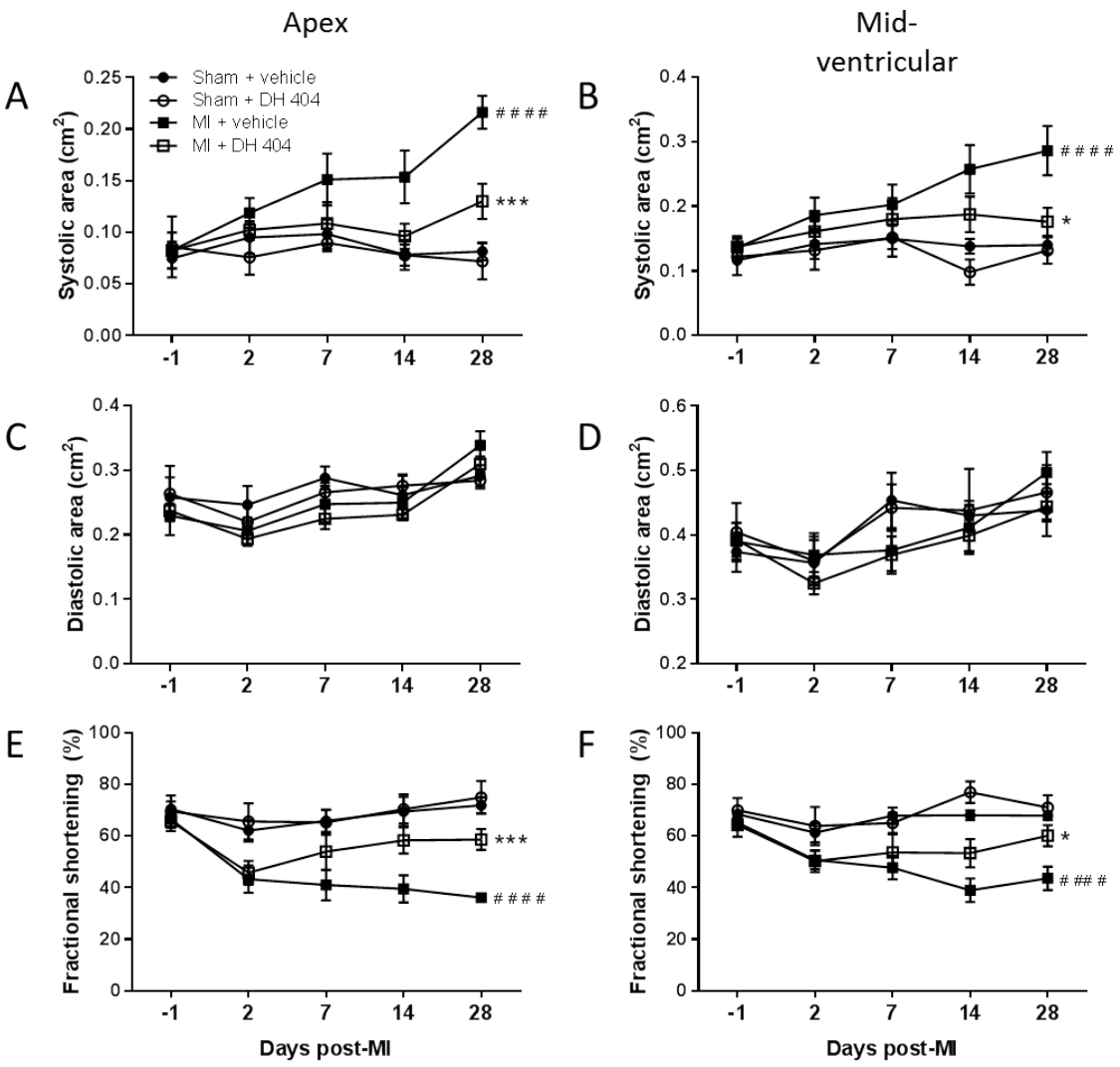

Figure 1. Serial echocardiographic data in rats. Systolic area (A, B), diastolic area (C, D) and fractional shortening (E, F) were measured before and serially over 28 days post-surgery in sham (n=5-6) and rats undergoing MI (n=8) with DH404 or vehicle. Apical echocardiography data is presented on the left panels (A, C, E) and mid-ventricular data on the right (B, D, F). Data are presented as mean ± SEM. Two-way ANOVA was used to determine differences between sham and MI (####P<0.0001 vs. sham) and between MI vehicle and MI + DH404 (*P<0.05, ***P<0.001).

Effect of DH404 on infarct expansion and remodeling

In order to assess the effect of DH404 on infarct expansion, we examined infarct size as a proportion of LV area at day 28 on Milligan's trichrome stained sections. Heart weights (normalized to tibial length) were not different in any of the experimental groups. Infarct size was significantly reduced in DH404-treated animals compared with

vehicle-treated MI rats (Figure 2A, B). Collagen accumulation, as estimated by polarized light microscopy in picrosirius red stained sections, substantially increased after MI but was attenuated by DH404 treatment (Figure 2C, D).

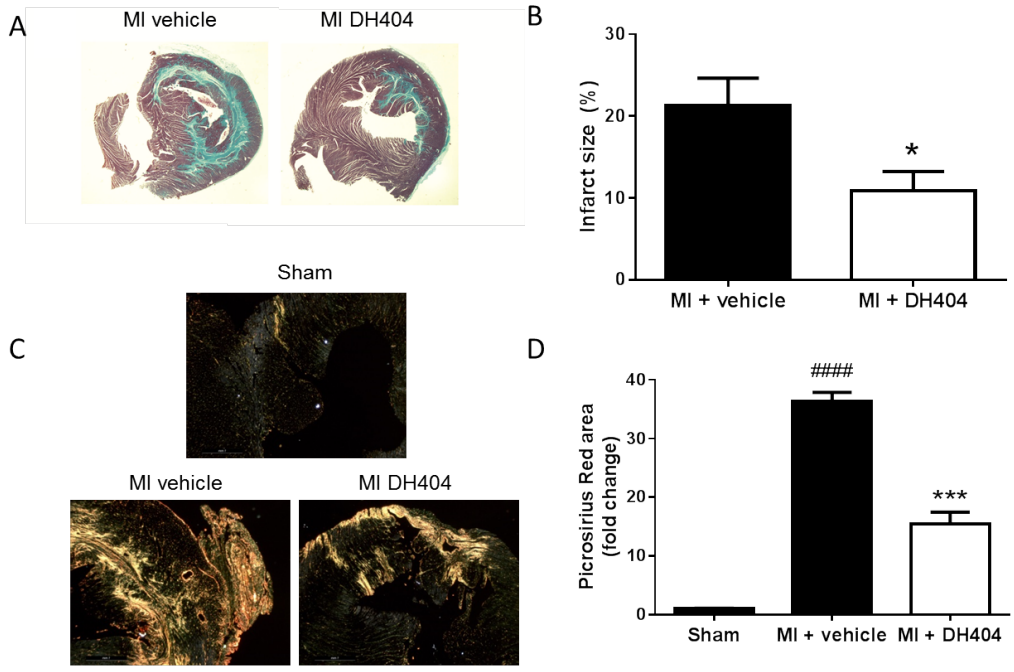

Figure 2. Effect of DH404 on infarct size at day 28 post MI (n=4-5). (A) Representative images and (B) summary data for infarct size. (C) Representative images and (B) summary analysis of picrosirius red stained heart sections demonstrating collagen are shown Data are shown as mean ± SEM. *P<0.05, ***P<0.001 versus MI + vehicle by Mann-Whitney or Kruskal-Wallis tests; ####P<0.0001 vs. sham.

Fibronectin, a key marker of fibrosis, was elevated up to 6-fold in the myocardium of the MI group compared to sham-operated hearts. However, this increase was more than halved in the animals receiving DH404 (Figure 3A), with a similar trend also being observed in protein expression (Figure 3B). Markers of heart failure, ANP and sarco-endoreticuloplasmic Ca^{2+} ATPase 2A (SERCA-2) expression [28] were increased and decreased respectively at day 28 post MI, and both were normalized by DH404 treatment (Figure 3C and D).

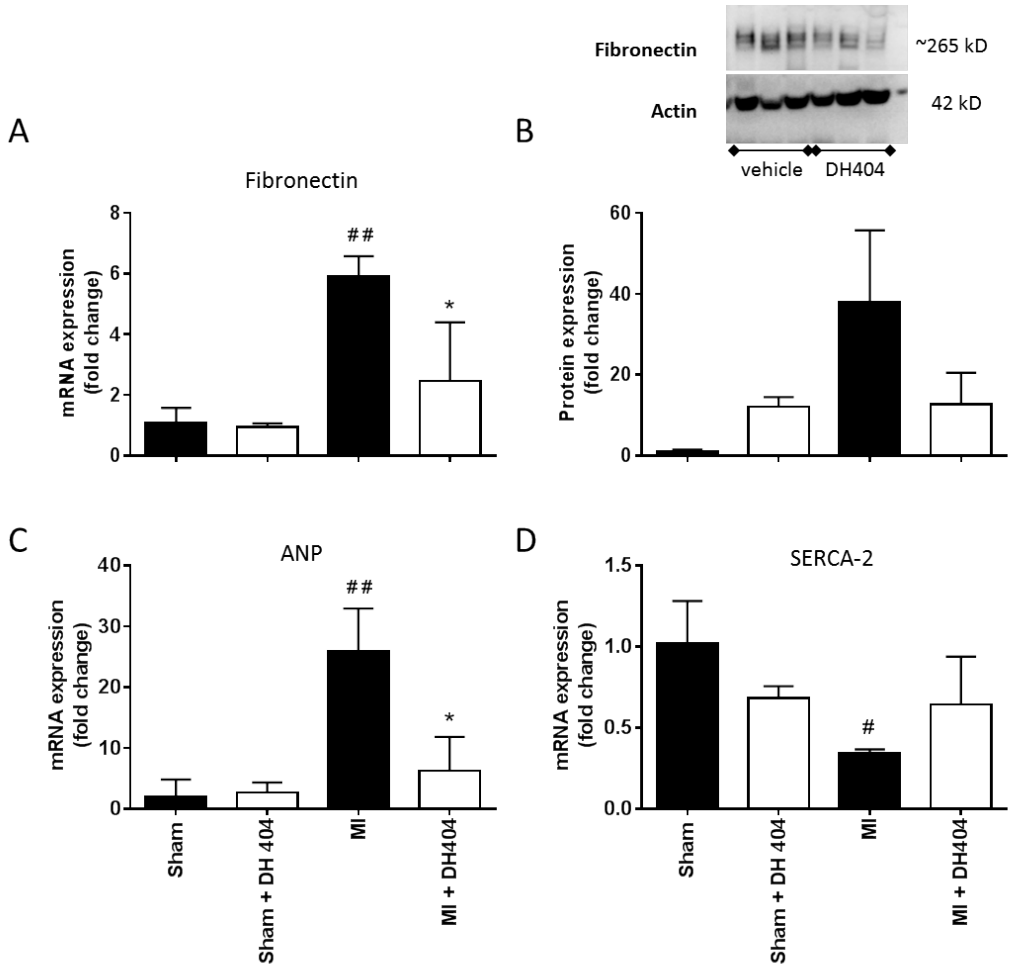

Figure 3. mRNA and protein expression of fibronectin (A,B) and mRNA expression of ANP (C) and SERCA-2 (D) in heart homogenates from sham and MI rats (n=3) treated with vehicle or DH404. Expression was normalized to beta-actin and expressed relative to sham-vehicle group. Data are presented as mean ± SEM. Statistical analysis was performed by Kruskal-Wallis test. $^{\#}P<0.05$, $^{\#\#}P<0.01$, $^{\#\#\#}P<0.001$ vs. sham vehicle, **P<0.01 vs. MI vehicle.

Effect of DH404 on redox signalling that underpins chronic remodeling post MI

Nrf2 is a well-known master regulator of antioxidant enzymes via transcriptional regulation of the antioxidant response element [29]. In preliminary studies we found that Nrf2 activation resulted in upregulated mRNA expression of known downstream antioxidant-associated targets including NAD(P)H:quinone oxidoreductase 1, the GSH regulating genes, glutamate-cysteine ligase complex catalytic subunit and glutathione S-

transferase, thioredoxin (Trx) regulating genes (Trx1, Trx1 reductase and peroxiredoxin) and sulfiredoxin (Table1).

Table 1. mRNA expression in Nrf2 target genes after acute DH404 administration in hearts of rats

Gene	DH404 (fold change)	SEM	P value
NADPH quinone oxidoreductase 1 (Nqo1)	1.68	0.16	0.0028
GCL catalytic subunit	2.17	0.08	<0.0001
Glutathione S-transferase 1	1.98	0.17	0.0004
Thioredoxin reductase 1	1.33	0.04	0.0001
Peroxiredoxin	1.19	0.05	0.0107
Thioredoxin 1	1.20	0.03	0.0005
Sulfiredoxin 1	2.24	0.21	0.0002

Data = mean ± SEM, presented as fold change from vehicle-treated rats; n= 6 per group.

Given known Nrf-2 dependence of enzymes involved in regulating glutathionylation [30], we examined the effect of DH404 administration on total protein glutathionylation detected by anti-glutathione in non-reduced rat heart homogenates. We found no difference in total glutathionylation across any of the treatment groups (Figure 4A, B). However, we were particularly interested in glutathionylation of eNOS as this redox modification mediates eNOS uncoupling, resulting in a dramatic switch from NO to superoxide production [31, 32] and is a strong candidate to play a role in ROS-dependent adverse cardiac remodeling [33]. While eNOS glutathionylation was detected at almost double the pre MI levels in vehicle-treated control animals at day 28, this increase was completely abrogated by treatment with DH404 (Figure 4C, D).

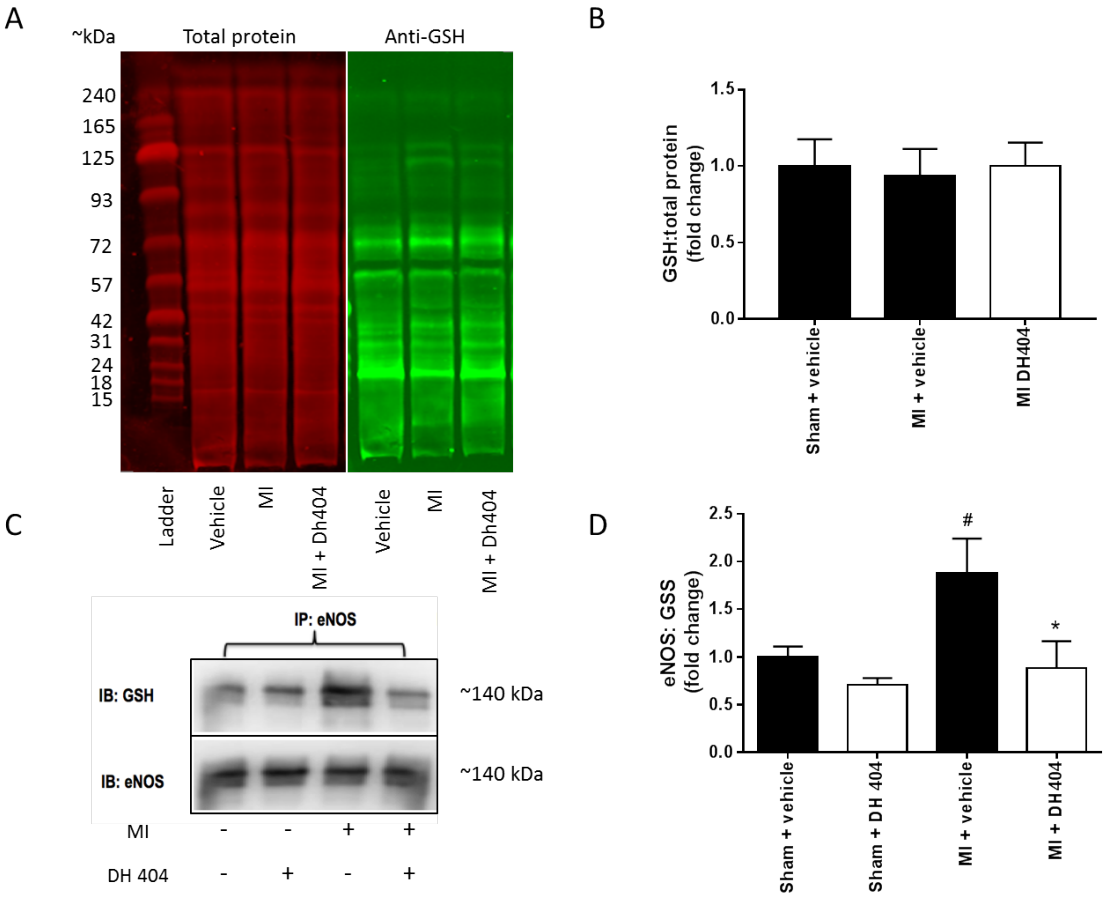

Figure 4. Total glutathionylation (GSH) (A, B) and eNOS-specific (C, D) glutathionylation (eNOS-GSS) measured by immunoprecipitation in heart homogenates from sham and MI vehicle and DH404 treated rats (n=3). Data presented as mean ± SEM. Statistical analysis by Kruskal-Wallis test. *P<0.05 vs. MI vehicle, #P<0.05 vs. sham vehicle. IP= immunoprecipitate; IB= immunoblot.

Given that eNOS glutathionylation has been reported to substantially reduce NO generation and augment superoxide production[31] and is increased after AngII treatment [34], we investigated the role of DH404 on NO and superoxide production in H9C2 rat cardiomyocytes treated with AngII, to mimic the neurohormonal abnormalities seen in heart failure patients, or vehicle control. In these cells eNOS glutathionylation followed the same pattern as for the heart tissue, as like MI, eNOS GSS tended to increase after AngII treatment and returned to baseline after DH404 but this failed to reach statistical significance (eNOS:GSS fold change: vehicle 1.00±0.09, AngII 2.85±1.26, AngII + DH404 1.65±0.50, P>0.05 by 1-way ANOVA, n=6). Importantly, AngII

treatment caused an increase in superoxide production which was attenuated by DH404 (Figure 5A) and this was associated with reduced NO production after AngII that was restored by DH404 (Figure 5B).

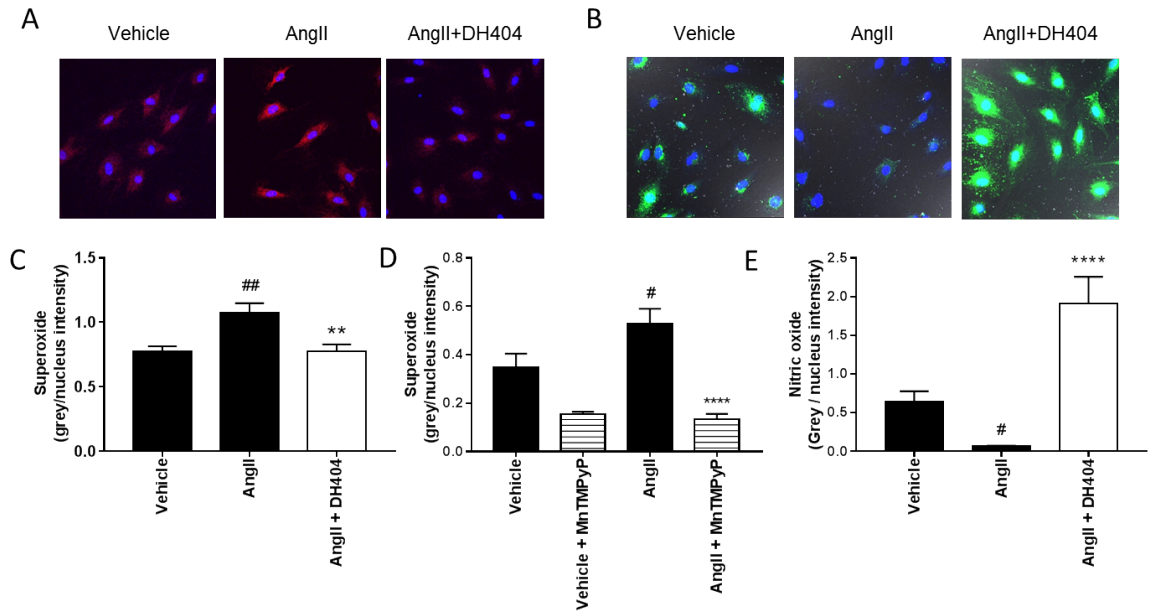

Figure 5. Representative confocal images of cells showing superoxide production (A, red) and NO production (B, green), with cell nuclei shown by DAPI stain (A,B, blue). DH404 attenuates AngII-induced superoxide production (C), and this was confirmed to be superoxide, rather than another species as superoxide dismutase mimetic MnTMPyP abolished the component attributed to increase by AngII (D). DH404 also restores NO production following NO-induced impaired NO generation (E) in H9C2 rat cardiomyocytes (n=14-24 experiments) . Data presented as mean ± SEM. Statistical analysis by one-way ANOVA. **P<0.01, ****P<0.0001 vs. AngII; $^{\#}$P<0.05, $^{\#\#}$P<0.01 vs. vehicle.

Mechanism for DH404 effects on eNOS uncoupling

Given the protective effects of DH404 on eNOS-GSS, we studied expression of Grx1, the enzyme akin to a phosphatase, which facilitates de-glutathionylation. DH404 administration did not significantly alter expression of Grx1 in rat hearts at 28 days post MI (fold change: sham vehicle 1.00±0.230, MI vehicle 0.97±0.10, MI DH404 1.06±0.20; n=3; P>0.05 Student's t-test). Nevertheless, since Grx1 activation is currently believed

to occur via an *encounter reaction*, i.e. by translocation to its targets, we examined the effect of DH404 on eNOS-Grx1 interaction by co-immunoprecipitation. eNOS-Grx1 interaction was decreased in response to both MI (Figure 6A) and after AngII treatment in H9C2 cardiomyocytes (Figure 6B). DH404 increased eNOS-Grx1 interaction compared with vehicle control in both the rat heart s and in cardiomyocytes (Figure 6).

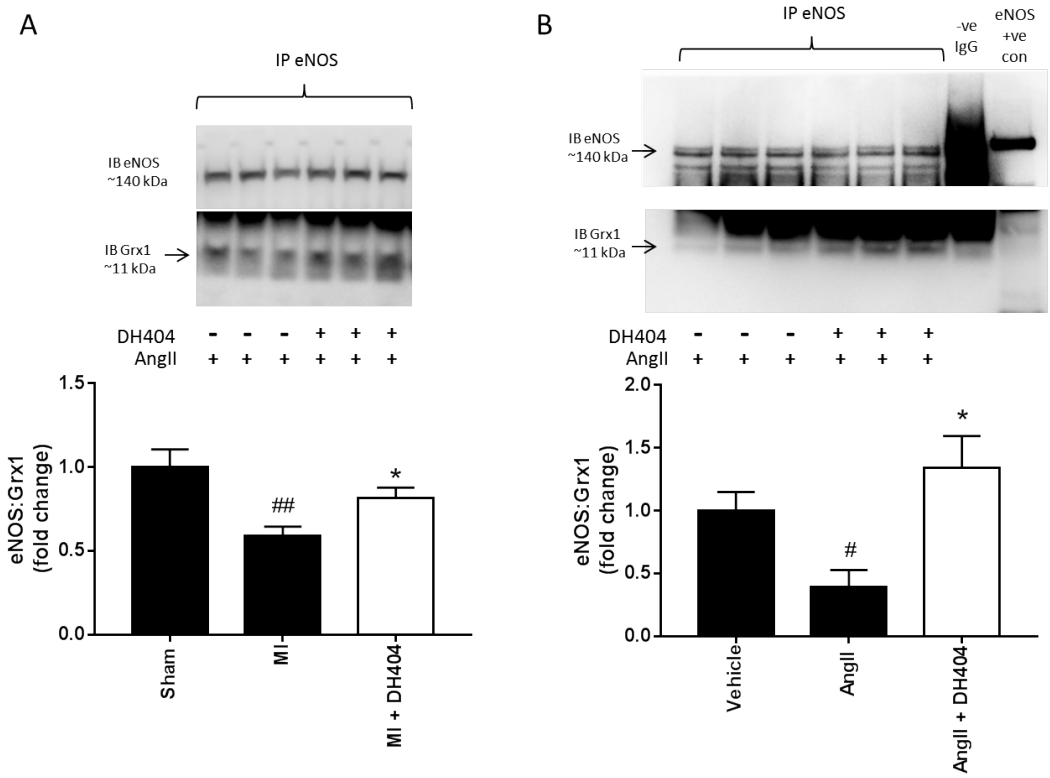

Figure 6. Co-immunoprecipitation (IP) of eNOS and Grx1. eNOS immunoprecipitate was immunoblotted (IB) for Grx1. Densitometry data was normalized to eNOS expression in rat hearts (A, n=3) and AngII-treated H9C2 neonatal rat cardiomyocytes (B, n=3) in the absence or presence of DH404. Data are shown as mean ±SEM. Statistical analysis performed by Kruskal-Wallis test. *P<0.05 vs. sham or vehicle, #P<0.05, ##P<0.01 vs. MI or AngII.

To elucidate whether the DH404 induced increase in eNOS-Grx1 interaction was functionally involved in improved eNOS coupling, we investigated whether the augmented NO production post-DH404 in rat cardiomyocytes was affected by Grx1 knockdown. After transfecting cardiomyocytes with Grx1 siRNA we confirmed Grx1 knockdown (KD) by ~10-fold reduction in Grx1 protein expression. This resulted in a

reduction in NO generation compared with control cells transfected with non-specific siRNA (Figure 7), suggesting that Grx1 is involved in the de-glutathionylation of eNOS after DH404 treatment.

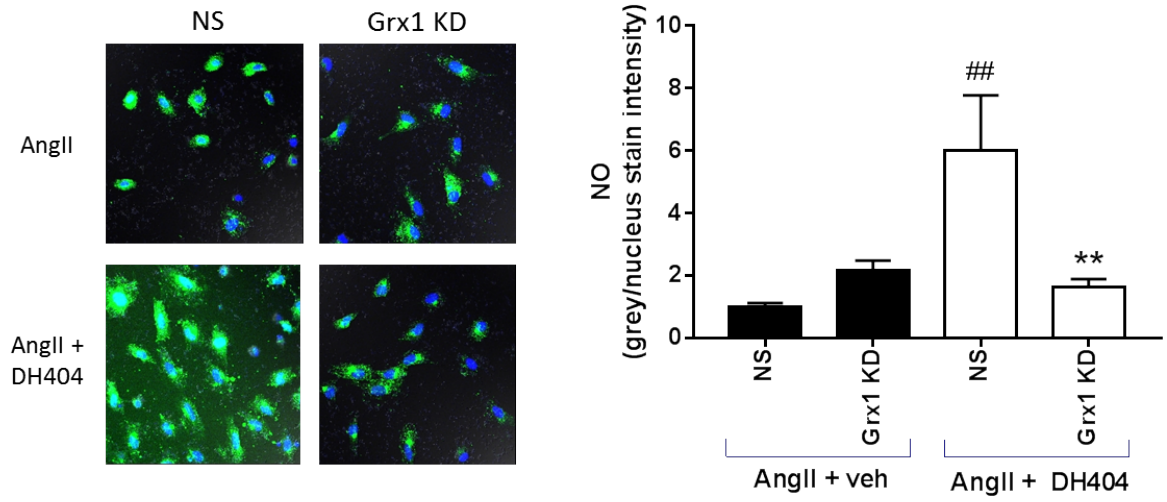

Figure 7. The augmented NO production by DH404 in AngII-treated H9C2 cells (n=12-24), transfected with non-specific (NS) siRNA, was abolished in cells transfected with Grx1 siRNA (Grx1 KD). Data presented as mean ± SEM and analysed by one-way ANOVA with Bonferroni post-hoc analysis. ##P<0.01 vs. vehicle, **P<0.01 vs. NS.

Discussion

In this study, we have demonstrated, for the first time, that the oral bardoxolone analogue DH404 is protective against the chronic adverse remodeling occurring over the weeks post MI in a rat model. We have observed important functional effects against infarct expansion, end-systolic dimensions, and contractile function. The finding that DH404 protects against eNOS glutathionylation, the molecular switch of the enzyme's uncoupling [31], suggests a new mechanism of benefit in ROS-dependent cardiovascular disease states. Overall, our results strongly support the therapeutic potential of DH404 in protecting against post MI cardiomyopathy and heart failure,

which remains a major cause of morbidity despite advancements in primary percutaneous coronary intervention and early reperfusion for acute MI.

Despite the known role of ROS in heart failure, general antioxidants such as Vitamin E have failed to demonstrate clinical benefit in large trials [35]. This is partially attributable to difficulties of such supplements to penetrate cellular micro domains that are home to tightly regulated redox signaling. The caveolae are an excellent example of this. These flask-like invaginations of the plasma membrane provide a structural platform for regulated function of membrane proteins [36]. The enrichment of these micro domains with eNOS and NADPH oxidase facilitates receptor-coupled physiological signalling by these enzymes. However, in pathophysiological states, it also allows focal dysregulated ROS production that can inhibit the function of important membrane proteins that co-localize in caveolae such as ion channels, the Na^+-K^+ pump [36, 37] and eNOS [31]. We hypothesized that Nrf2 activation by DH404 may influence redox-mediated dysregulation of caveolar proteins during the remodeling phase post MI, and focused on eNOS as both a sensor and effector molecule in redox-dependent signalling cascade [38]., We report, for the first time to our knowledge, that MI is associated with marked elevations in eNOS glutathionylation, a molecular event highly likely to contribute to redox-dependent adverse remodeling. DH404 protection against eNOS glutathionylation and uncoupling may be key in its beneficial effects against adverse remodeling since this molecular switch is causally associated with an increase in NO bioavailability, and a reduction in superoxide levels; shifting the equilibrium in NO/redox-dependent signaling back towards physiological levels (Figure 8). Although not directly tested in this study, we predict that this occurs within the caveolae,a signalling compartment that has over 200 redox-sensitive proteins, many of which are

either ion channels or pumps, or are critical to a multitude of cellular signaling pathways [39].

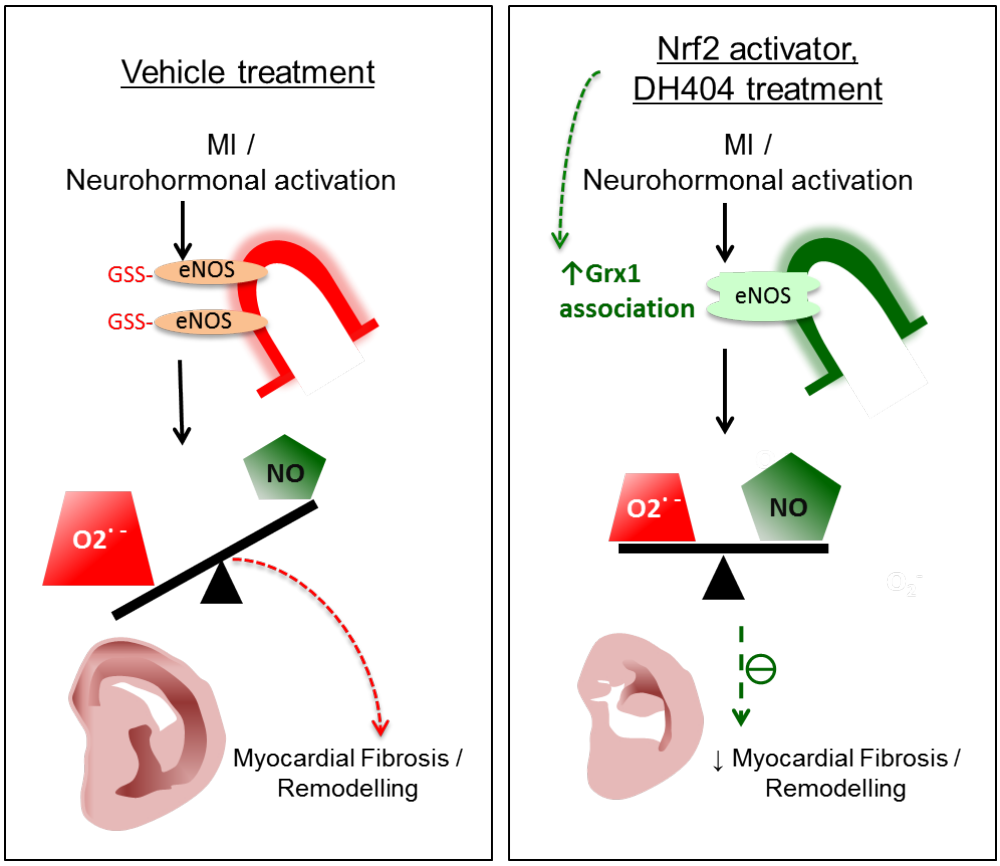

Figure 8. Summary of the new mechanism contributing to the protective effect of DH404 against redox-mediated adverse remodeling post MI, as suggested by our current study. Myocardial remodeling post MI is mediated by dysfunctional redox signaling. The uncoupling of eNOS, mediated by glutathionylation (eNOS-GSS) results in increased superoxide ($O_2^{\cdot-}$) and decreased NO, and is a likely contributor to ROS-mediated remodeling. Nrf2 activation by DH404 results in increased co-immunoprecipitation of Grx1 with eNOS, and an associated decrease in eNOS-GSS. Although the mechanism for this remains to be elucidated, we postulate that this signaling event plays an important role in the protective effect of DH404 on myocardial remodeling post MI injury.

Although we clearly demonstrate that DH404 protects against eNOS glutathionylation in the myocardium undergoing remodeling, the mechanism for this was not immediately obvious. DH404 activates Nrf2, which is under regulatory control by the repressor molecule, Keap1. However when stimulated by bardoxolone, Nrf2 undergoes translocation to the nucleus where it transcriptionally regulates ARE [14, 15]. This

ultimately leads to the up regulation of a panel of redox-sensitive genes, such as Nqo1[40, 41], sulfiredoxin[42], Gstp1[41] and Grx1[40]. Although these enzymes are all known to have a role in cellular redox status, the specific role of these enzymes in protecting caveolar proteins from pathophysiological ROS is not well understood. Indeed, Grx1, the most valid candidate for decreasing glutathionylation, is classically considered a cytosolic enzyme. However, we and others have previously demonstrated it to interact with and deglutathionylate two resident caveolar proteins, the Na^+-K^+ pump [27, 43, 44] and eNOS [31, 32, 45]. The mechanism of regulation of Grx1 translocation and interaction with caveolar proteins is poorly understood.

Although we found no significant increase in Grx1 expression to explain the protection against MI-induced eNOS glutathionylation, oral DH404 increased the co-immunoprecipitation of Grx1 with eNOS. This reflects enhanced functional interaction of Grx1 to its caveolar target. Glutaredoxin is known to deglutathionylate eNOS, facilitating NO production [32, 45]. The role of Grx1 in DH404 protection of eNOS glutathionylation and uncoupling was strongly supported by data from a reductionist cell culture model. Here, the ability of DH404 to reverse AngII induced eNOS uncoupling in H9C2 cardiomyocytes was lost by silencing Grx1. Together our data point to a new mechanism, for DH404 to protect the myocardium via enhancing the functional interaction of glutaredoxin with eNOS and decreasing glutathionylation. The reestablishment of NO/superoxide balance during the recovery phases post MI likely contributes to the observed protective effect of DH404.

In addition to the new molecular mechanistic insights unraveled in this study, it is important to consider the implications of the functional findings for clinical translation and potential management of heart failure in post MI patients. DH404 had profound effects in protecting against the increase in LV end-systolic dimensions in the

remodeling period. End systolic dimensions are recognized as one of the most important surrogate markers in human clinical trials post MI, and are powerful predictors of mortality [46]. The associated improvements in fractional shortening, ANP and fibronectin expression, and the trend to attenuated remodeling-induced SERCA-2 expression [47], all support the functional benefits. SERCA-2 is also recognized as being sensitive to post-translational modification by glutaredoxin [48] however we did not address this in this study. The translational potential of the findings in this study are particularly enticing given the substantial clinical incidence of heart failure in patients surviving MI, as well as the current availability of Nrf2 activating therapies for human trials [18, 49].

A valid consideration regarding the potential application of Nrf2 activation to human heart failure post MI is the observation in the Phase 3 BEACON Trial of patients with diabetes and stage 4 renal failure that bardoxolone methyl was associated with a higher rate of heart failure events (occurring in 8.8%) compared with placebo (occurring in 5.0%) [49]. Two major risk factors were shown to predict heart failure events in BEACON study: baseline BNP>200 pg/ml and previous hospitalization for heart failure [50]. Intriguingly, this appears to result from a reduction in urine volume and sodium excretion in the early weeks after commencing therapy, consistent with preclinical studies that had demonstrated an effect of bardoxolone methyl in modulating endothelin expression in the kidneys [50] [51], and is independent of Nrf2 signalling. This postulated mechanism, impacting negatively on a very select population of patients identified to be at high risk of decompensated heart failure after small alterations in sodium excretion, does not preclude a possible direct beneficial effect of bardoxolone methyl or related compounds on redox-dependent myocardial remodeling in patients

with normal renal function. Importantly, in patients not susceptible to fluid overload, the risk of bardoxolone–precipitated heart failure was similar to controls (2%) [50].

Since the premature termination of the BEACON study due to the higher rate of heart failure events, a number of other disease populations have received Bardoxolone methyl, or its close structural analogue RTA 408 in Phase II studies [52], including pulmonary hypertension (NCT02036970), where initial results are promising and Phase III development is being initiated with bardoxolone methyl [53], and with RTA 408 for mitochondrial myopathy (NCT02255422), Friedrich's ataxia (NCT02255435) [54], or radiation-induced tissue damage during cancer chemotherapy (NCT02142959) [54]. In these populations, less susceptible to subtle changes in sodium excretion, no issues with heart failure have been raised. Thus, it seems that our findings may be translated to human studies in the population of patients with impaired LV function post-ST elevation, excluding those with significant renal dysfunction.

In conclusion, the Nrf2 activator, DH404 was protective against infarct expansion and maladaptive remodeling post MI in rats when administered from day 2 post injury. The associated decrease in redox modification of eNOS in DH404-treated animals suggests that the agent is able to protect against dysregulated oxidative signaling in the caveolae micro domain in a manner that may benefit functionally important, redox-sensitive membrane biomolecules. This study provides a rationale for further studies in pre-clinical models and human studies where cardiac remodeling post MI remains an undertreated major problem.

Acknowledgements:

The authors would like to acknowledge Sarah Tandy for invaluable technical assistance with the myocardial infarction model. GAF is funded by NHMRC Career Development Fellowship APP 1062262 and a Heart Foundation Australia Future Leader Fellowship and Heart Research Australia. RB is funded by a Heart Foundation Future Leader fellowship. RHR is a NHMRC Senior Research Fellow (APP1059960). KJB is funded by a Heart Research Australia ECR grant.

References

[1]. Lopez, A.D., et al., Global and regional burden of disease and risk factors, 2001: systematic analysis of population health data. Lancet, 367. (9524) (2006), pp. 1747-57.
[2]. Konstam, M.A., et al., Left ventricular remodeling in heart failure: current concepts in clinical significance and assessment. JACC Cardiovasc Imaging, 4. (1) (2011), pp. 98-108.
[3]. Wang, Q.D., et al., Pharmacological possibilities for protection against myocardial reperfusion injury. Cardiovasc Res, 55. (1) (2002), pp. 25-37.
[4]. Ambrosio, G. and I. Tritto, Reperfusion injury: experimental evidence and clinical implications. Am Heart J, 138. (2 Pt 2) (1999), pp. S69-75.
[5]. Shattock, M.J., Phospholemman: its role in normal cardiac physiology and potential as a druggable target in disease. Curr Opin Pharmacol, 9. (2) (2009), pp. 160-6.
[6]. Lefer, A.M., et al., Role of endothelial dysfunction in the pathogenesis of reperfusion injury after myocardial ischemia. FASEB journal : official publication of the Federation of American Societies for Experimental Biology, 5. (7) (1991), pp. 2029-34.
[7]. Burgoyne, J.R., et al., Redox signaling in cardiac physiology and pathology. Circ Res, 111. (8) (2012), pp. 1091-106.
[8]. Uraizee, A., et al., Failure of superoxide dismutase to limit size of myocardial infarction after 40 minutes of ischemia and 4 days of reperfusion in dogs. Circulation, 75. (6) (1987), pp. 1237-48.
[9]. Venturini, C.M., et al., The Antioxidant, N-(2-mercaptopropionyl)-glycine (MPG), Does Not Reduce Myocardial Infarct Size in an Acute Canine Model of Myocardial Ischemia and Reperfusion. J Thromb Thrombolysis, 5. (2) (1998), pp. 135-141.
[10]. Flaherty, J.T., et al., Recombinant human superoxide dismutase (h-SOD) fails to improve recovery of ventricular function in patients undergoing coronary angioplasty for acute myocardial infarction. Circulation, 89. (5) (1994), pp. 1982-91.
[11]. Liby, K.T., M.M. Yore, and M.B. Sporn, Triterpenoids and rexinoids as multifunctional agents for the prevention and treatment of cancer. Nat Rev Cancer, 7. (5) (2007), pp. 357-369.

[12]. Cleasby, A., et al., Structure of the BTB domain of Keap1 and its interaction with the triterpenoid antagonist CDDO. PLoS One, 9. (6) (2014), pp. e98896.
[13]. Huerta, C., et al., Characterization of novel small-molecule NRF2 activators: Structural and biochemical validation of stereospecific KEAP1 binding. Biochim Biophys Acta, 1860. (11 Pt A) (2016), pp. 2537-52.
[14]. Espinosa-Diez, C., et al., Antioxidant responses and cellular adjustments to oxidative stress. Redox Biol, 6. (2015), pp. 183-97.
[15]. McMahon, M., et al., Dimerization of substrate adaptors can facilitate cullin-mediated ubiquitylation of proteins by a "tethering" mechanism: a two-site interaction model for the Nrf2-Keap1 complex. J Biol Chem, 281. (34) (2006), pp. 24756-68.
[16]. Wang, Y.Y., et al., Bardoxolone methyl (CDDO-Me) as a therapeutic agent: an update on its pharmacokinetic and pharmacodynamic properties. Drug Des Devel Ther, 8. (2014), pp. 2075-88.
[17]. Chin, M., et al., Bardoxolone methyl analogs RTA 405 and dh404 are well tolerated and exhibit efficacy in rodent models of Type 2 diabetes and obesity. Am J Physiol Renal Physiol, 304. (12) (2013), pp. F1438-46.
[18]. Pergola, P.E., et al., Bardoxolone Methyl and Kidney Function in CKD with Type 2 Diabetes. New England Journal of Medicine, 365. (4) (2011), pp. 327-336.
[19]. Ichikawa, T., et al., Dihydro-CDDO-trifluoroethyl amide (dh404), a novel Nrf2 activator, suppresses oxidative stress in cardiomyocytes. PLoS One, 4. (12) (2009), pp. e8391.
[20]. Xing, Y., et al., Triterpenoid dihydro-CDDO-trifluoroethyl amide protects against maladaptive cardiac remodeling and dysfunction in mice: a critical role of Nrf2. PLoS One, 7. (9) (2012), pp. e44899.
[21]. Bhindi, R., et al., Rat models of myocardial infarction. Pathogenetic insights and clinical relevance. Thromb Haemost, 96. (5) (2006), pp. 602-10.
[22]. Noyan-Ashraf, M.H., et al., GLP-1R agonist liraglutide activates cytoprotective pathways and improves outcomes after experimental myocardial infarction in mice. Diabetes, 58. (4) (2009), pp. 975-83.
[23]. Junqueira, L.C., G. Bignolas, and R.R. Brentani, Picrosirius staining plus polarization microscopy, a specific method for collagen detection in tissue sections. Histochem J, 11. (4) (1979), pp. 447-55.
[24]. Livak, K.J. and T.D. Schmittgen, Analysis of relative gene expression data using real-time quantitative PCR and the 2(-Delta Delta C(T)) Method. Methods, 25. (4) (2001), pp. 402-8.
[25]. Reisman, S.A., et al., Increased Nrf2 activation in livers from Keap1-knockdown mice increases expression of cytoprotective genes that detoxify electrophiles more than those that detoxify reactive oxygen species. Toxicol Sci, 108. (1) (2009), pp. 35-47.
[26]. Liu, C.C., et al., Susceptibility of beta1 Na+-K+ pump subunit to glutathionylation and oxidative inhibition depends on conformational state of pump. J Biol Chem, 287. (15) (2012), pp. 12353-64.
[27]. Figtree, G.A., et al., Reversible oxidative modification: a key mechanism of Na+-K+ pump regulation. Circ Res, 105. (2) (2009), pp. 185-93.
[28]. Hasenfuss, G., et al., Relation between myocardial function and expression of sarcoplasmic reticulum Ca(2+)-ATPase in failing and nonfailing human myocardium. Circ Res, 75. (3) (1994), pp. 434-42.

[29]. Gorrini, C., I.S. Harris, and T.W. Mak, Modulation of oxidative stress as an anticancer strategy. Nat Rev Drug Discov, 12. (12) (2013), pp. 931-47.
[30]. Ramprasath, T., et al., Regression of oxidative stress by targeting eNOS and Nrf2/ARE signaling: a guided drug target for cardiovascular diseases. Curr Top Med Chem, 15. (9) (2015), pp. 857-71.
[31]. Chen, C.A., et al., S-glutathionylation uncouples eNOS and regulates its cellular and vascular function. Nature, 468. (7327) (2010), pp. 1115-8.
[32]. Galougahi, K.K., et al., Glutathionylation mediates angiotensin II-induced eNOS uncoupling, amplifying NADPH oxidase-dependent endothelial dysfunction. J Am Heart Assoc, 3. (2) (2014), pp. e000731.
[33]. Takimoto, E. and D.A. Kass, Role of oxidative stress in cardiac hypertrophy and remodeling. Hypertension, 49. (2) (2007), pp. 241-8.
[34]. Galougahi, K.K., et al., Glutathionylation Mediates Angiotensin II‐Induced eNOS Uncoupling, Amplifying NADPH Oxidase‐Dependent Endothelial Dysfunction. Journal of the American Heart Association, 3. (2) (2014), pp. e000731.
[35]. Yusuf, S., et al., Vitamin E supplementation and cardiovascular events in high-risk patients. The Heart Outcomes Prevention Evaluation Study Investigators. N Engl J Med, 342. (3) (2000), pp. 154-60.
[36]. Patel, H.H. and P.A. Insel, Lipid rafts and caveolae and their role in compartmentation of redox signaling. Antioxid Redox Signal, 11. (6) (2009), pp. 1357-72.
[37]. Figtree, G.A., et al., Oxidative regulation of the Na^+-K^+ pump in the cardiovascular system. Free Radic Biol Med, 53. (12) (2012), pp. 2263-2268.
[38]. Crabtree, M.J., et al., Integrated redox sensor and effector functions for tetrahydrobiopterin- and glutathionylation-dependent endothelial nitric-oxide synthase uncoupling. J Biol Chem, 288. (1) (2013), pp. 561-9.
[39]. Wypijewski, K.J., et al., Identification of caveolar resident proteins in ventricular myocytes using a quantitative proteomic approach: dynamic changes in caveolar composition following adrenoceptor activation. Mol Cell Proteomics, 14. (3) (2015), pp. 596-608.
[40]. Liu, X., et al., The novel triterpenoid RTA 408 protects human retinal pigment epithelial cells against H2O2-induced cell injury via NF-E2-related factor 2 (Nrf2) activation. Redox Biology, 8. (2016), pp. 98-109.
[41]. Walsh, J., et al., Identification and quantification of the basal and inducible Nrf2-dependent proteomes in mouse liver: biochemical, pharmacological and toxicological implications. J Proteomics, 108. (2014), pp. 171-87.
[42]. Soriano, F.X., et al., Transcriptional regulation of the AP-1 and Nrf2 target gene sulfiredoxin. Mol Cells, 27. (3) (2009), pp. 279-82.
[43]. Galougahi, K.K., et al., β3-Adrenoceptor activation relieves oxidative inhibition of the cardiac Na+-K+ pump in hyperglycemia induced by insulin receptor blockade. American Journal of Physiology-Cell Physiology, 309. (5) (2015), pp. C286-C295.
[44]. Karimi Galougahi, K., et al., β3 adrenergic stimulation restores nitric oxide/redox balance and enhances endothelial function in hyperglycemia . Journal of the American Heart Association, in press. (accepted Jan 7) (2016), pp.
[45]. Chen, C.A., et al., Redox modulation of endothelial nitric oxide synthase by glutaredoxin-1 through reversible oxidative post-translational modification. Biochemistry, 52. (38) (2013), pp. 6712-23.

[46]. White, H.D., et al., Left ventricular end-systolic volume as the major determinant of survival after recovery from myocardial infarction. Circulation, 76. (1) (1987), pp. 44-51.
[47]. Bostjancic, E., N. Zidar, and D. Glavac, MicroRNAs and cardiac sarcoplasmic reticulum calcium ATPase-2 in human myocardial infarction: expression and bioinformatic analysis. BMC Genomics, 13. (2012), pp. 552.
[48]. Adachi, T., et al., S-Glutathiolation by peroxynitrite activates SERCA during arterial relaxation by nitric oxide. Nat Med, 10. (11) (2004), pp. 1200-7.
[49]. de Zeeuw, D., et al., Bardoxolone methyl in type 2 diabetes and stage 4 chronic kidney disease. N Engl J Med, 369. (26) (2013), pp. 2492-503.
[50]. Chin, M.P., et al., Risk factors for heart failure in patients with type 2 diabetes mellitus and stage 4 chronic kidney disease treated with bardoxolone methyl. J Card Fail, 20. (12) (2014), pp. 953-8.
[51]. Chin, M.P., et al., Mechanisms contributing to adverse cardiovascular events in patients with type 2 diabetes mellitus and stage 4 chronic kidney disease treated with bardoxolone methyl. Am J Nephrol, 39. (6) (2014), pp. 499-508.
[52]. Schmidt, H.H., et al., Antioxidants in Translational Medicine. Antioxid Redox Signal, 23. (14) (2015), pp. 1130-43.
[53]. Oudiz, R.J., et al. *Bardoxolone Methyl Evaluation in Patients with Pulmonary Arterial Hypertension (PAH): Initial Data Report from LARIAT: A Phase 2 Study of Bardoxolone Methyl in PAH Patients on Stable Background Therapy* CHEST Annual Meeting, 2015, Montreal, Canada; Available from: http://reatapharma.com/wp-content/uploads/2015/10/LARIAT_CHEST_Final.pdf.
[54]. https://clinicaltrials.gov. (accessed March 11, 2016), pp.